 <p>EUMETSAT NWP SAF NUMERICAL WEATHER PREDICTION</p>	<p>Report on MetOp-C AMSU-A, MHS and IASI radiance data quality.</p>	<p>Doc ID : NWPSAF-MO-TR-037 Version : 1.3 Date : 17/02/2020</p>
--	---	--

Report on Metop-C AMSU-A, MHS and IASI radiance data quality.

Michael Cooke¹, Christina Köpken-Watts², Brett Candy¹, Laura Pitcher¹, Robin Faulwetter², Chawn Harlow¹, and Nigel Atkinson¹


¹ Met Office, Exeter, United Kingdom;

² DWD, Offenbach, Germany

This documentation was developed within the context of the EUMETSAT Satellite Application Facility on Numerical Weather Prediction (NWP SAF), under the Cooperation Agreement dated 7 December 2016, between EUMETSAT and the Met Office, UK, by one or more partners within the NWP SAF. The partners in the NWP SAF are the Met Office, ECMWF, DWD and Météo France.


Copyright 2019, EUMETSAT, All Rights Reserved.

Change record			
Version	Date	Author / changed by	Remarks
1.0	20/11/19	Michael Cooke	Initial draft.
1.1	20/01/20	Christina Köpken-Watts	Revised draft. Addition of DWD results
1.2	10/02/20	Michael Cooke	Final version to check
1.3	17/02/20	Michael Cooke	Approved document

 <p>EUMETSAT NWP SAF NUMERICAL WEATHER PREDICTION</p>	<p>Report on MetOp-C AMSU-A, MHS and IASI radiance data quality.</p>	<p>Doc ID : NWPSAF-MO-TR-037 Version : 1.3 Date : 17/02/2020</p>
--	---	--

Contents

- 1. INTRODUCTION..... 3
- 2. DATA CHARACTERIZATION..... 4
 - 2.1. AMSU-A AND MHS INSTRUMENT CHARACTERISTICS AND DATA PROCESSING ... 4
 - 2.2. AMSU-A AND MHS MONITORING RESULTS 4
 - 2.3. IASI INSTRUMENT CHARACTERISTIC AND DATA PROCESSING..... 6
 - 2.4. IASI MONITORING RESULTS 6
- 3. DATA TIMELINESS 8
- 4. CONCLUSIONS 8
- 5. REFERENCES..... 10
- 6. FIGURES 12

 <p>EUMETSAT NWP SAF NUMERICAL WEATHER PREDICTION</p>	<p>Report on MetOp-C AMSU-A, MHS and IASI radiance data quality.</p>	<p>Doc ID : NWPSAF-MO-TR-037 Version : 1.3 Date : 17/02/2020</p>
--	---	--

1. Introduction


Meteorological operational satellite - C (Metop-C) was launched on 7th November 2018. It is the third and final satellite in the EUMETSAT Polar System (EPS) programme which began with the launch of Metop-A in 2006. Its payload consists of eight instruments including the Advanced Microwave Sounding Unit – A (AMSU-A), the Microwave Humidity Sounding (MHS) instrument and the Infrared Atmospheric Sounding Interferometer (IASI). Since Metop-C was commissioned, EUMETSAT has simultaneously operated three Metop satellites. Initially, the three satellites were equally spaced around their orbit about 120° apart, but early in 2020 the satellites will be moved to a Trident configuration with Metop-B and -C 180° apart and Metop-A at 90° between them. Metop-A will reach its end of life in 2022 leaving Metop-B and -C.

Since the launch of NOAA-15 in 1998 the Advanced Microwave Sounding Unit (AMSU), Microwave Humidity Sounder (MHS) and High-resolution InfraRed Sounder (HIRS) have been a key part in the vertical sounding of the atmosphere for NWP models (English et al., 2000). The AMSU-A instruments are onboard the POES (NOAA 15-19) and Metop (Metop A-C) satellite series while AMSU-B was the humidity sounder on NOAA 15-17 and was replaced with MHS from NOAA 18 onwards and is on all the Metop satellites. These microwave instruments have delivered significant benefit in many operational global and regional data assimilation systems (e.g. in Joo et al., 2012) and only recently studies conducted by all major global weather services have underlined the importance of these microwave data, and also microwave imagers, for the current quality of NWP (RFI workshop report, 2019).

Hyperspectral IR sounding data from space first became available when the Atmospheric InfraRed Sounder (AIRS; Chahine et al., 2006) was launched on the Aqua satellite as an experimental mission in 2002. AIRS is a grating spectrometer with 2378 channels in the visible and infrared. It is now regularly assimilated at NWP centres (e.g. Cameron et al., 2005). The Infrared Atmospheric Sounding Interferometer (IASI) became the first operational hyperspectral IR interferometer when it was launched by EUMETSAT on the first Metop satellite in October 2006. IASI data have been assimilated at the Met Office since 27 November 2007 and at DWD since July 2014. Details on the initial implementation of IASI at the Met Office can be found in Hilton et al. (2009) with NWP impact trials showing that it had twice the impact of the AIRS instrument and an equivalent impact to a single AMSU-A combined with a single MHS instrument.

This report provides a quality assessment of the IASI, AMSU-A and MHS instruments on Metop-C, the last satellite in the EUMETSAT Polar System (EPS) series, which was launched on 7 November 2018. The report is focussing on a NWP user perspective and evaluates the data quality by comparing the observations to model equivalents from short-range forecasts using forward simulations with the fast radiative transfer model, RTTOV (Saunders et al. 2018). Such an evaluation is done in an operational data assimilation system and setup and is an essential first step for the subsequent operational assimilation of any new data in routine NWP applications. Prior to producing the monitoring results, the data are integrated into the technical processing steps and data specific quality control checks are implemented or adapted. Such data screening details may vary between centres and are described in Section 2 for both the Met Office and DWD before presentation of the respective results for AMSU-A, MHS and IASI. Overall results are summarized in Section 3.

It should be stressed that such data monitoring in a NWP context cannot evaluate the accuracy of the absolute calibration of an instrument as the NWP models themselves display model specific biases, e.g. in temperature and humidity fields, that also vary with region and height resulting in spectrally varying biases in radiance or brightness temperature space. Additionally, the radiative transfer employed is not bias free (see Saunders et al. 2013 for RTTOV evaluation). Biases are addressed in a NWP context with bias correction schemes, removing systematic differences between observations and models on broad scales. But despite NWP not being an absolute calibration reference, the NWP monitoring has proven to be a very powerful tool in checking for systematic noise patterns and complex or variable bias characteristics in satellite data (e.g. Booton, 2014; Köpken, 2004). NWP monitoring is now routinely contributing to the evaluation of instrument performances for new instruments at EUMETSAT, NOAA, JMA, CMA and other agencies as well as to their continuous near-real time performance monitoring (e.g. through the NWP SAF at

 <p>EUMETSAT NWP SAF NUMERICAL WEATHER PREDICTION</p>	<p>Report on MetOp-C AMSU-A, MHS and IASI radiance data quality.</p>	<p>Doc ID : NWPSAF-MO-TR-037 Version : 1.3 Date : 17/02/2020</p>
--	---	--

<https://www.nwpsaf.eu/site/monitoring/nrt-monitoring/>). To address some of the shortcomings relating to models also being non-perfect, the evaluation summarized here employs two independent and very different NWP systems from the Met Office and the German Weather Service DWD. The Met Office comparison uses the Unified Model (UM) at N1280 resolution (~10 km) with hybrid 4DVar and the DWD comparisons are based on the ICOSahedral Nonhydrostatic ICON+EnVar system at 13 km resolution.

2. Data Characterization

2.1. AMSU-A and MHS instrument characteristics and data processing

AMSU-A is a multi-channel microwave radiometer which has 15 discrete channels in the 23-90 GHz range. AMSU-A is a cross-track scanner with 30 steps and a swath width of about 2200 km. At the sub-satellite position the footprint size is 48 km. The data primarily provides information on atmospheric temperature. It gets secondary information about water in all its forms (excluding very small ice particles which are transparent at microwave frequencies) including in cloudy conditions. MHS operates in the 89-190 GHz region primarily providing information on atmospheric humidity. MHS is also sensitive to atmospheric temperature, cloud and surface conditions. MHS is a cross-track scanning, five channel microwave instrument with a footprint size of 16 km and a total swath width of about 2200 km.

At the Met Office the instruments are treated together, with the observations being mapped during pre-processing onto a single grid which involves mapping AMSU-A and MHS onto the HIRS grid (56 across track spots across a swath of 2200 km) for Metop-A and –B. For Metop-C MHS is mapped onto the AMSU-A grid (30 across track spots across a swath of 2250 km) as no HIRS instrument is flying on Metop-C. Level 0 direct broadcast data from AMSU-A and MHS are received locally and processed to calibrated radiances using the AAPP package (Atkinson, 2017). Global data are received via the EUMETCast service. The AAPP package performs the mapping and some initial quality control, evaluating general flags in the L1 data and excluding any unphysical observations.


At DWD, global data received via EUMETCast are evaluated. The instruments are each evaluated on their original grids without mapping. DWDs pre-processing also includes checks of flags provided in the L1 data as well as screening for unphysical brightness temperatures.

The presented evaluation from both centres uses the globally received data, but results are equally applicable to locally received data distributed through the DBNet as the consistency of both data sets is continuously monitored (e.g. NWPSAF DBNet monitoring, see <https://www.nwpsaf.eu/site/monitoring/dbnet/>).

2.2. AMSU-A and MHS monitoring results

To check the quality of the AMSU-A and MHS instruments on Metop-C, observed brightness temperatures (O or OBS) have been compared against simulated brightness temperatures from short-range forecast fields (noted as background, B or first guess, FG). At the Met Office, the background is a 3-9 hour forecast valid at the observation time based on the 6-hourly 4DVar cycle. At DWD a 3 hour first guess valid at the mid time of a 3 hour observation window is used, i.e. currently without interpolation to the actual observation time in this window. The instruments are also compared with the Metop-A and Metop-B instruments which are already being used operationally.

The comparisons are restricted to data screened for the influence of thick clouds and rain (i.e. rain, cloud water and ice emission, absorption and scattering effects) using a combination of several tests using either a combination of the observations themselves at various frequencies (channels) or also involving the first guess NWP estimates. Additionally, a so-called FG check excludes outlier observations. The tests employed

 <p>EUMETSAT NWP SAF NUMERICAL WEATHER PREDICTION</p>	<p>Report on MetOp-C AMSU-A, MHS and IASI radiance data quality.</p>	<p>Doc ID : NWPSAF-MO-TR-037 Version : 1.3 Date : 17/02/2020</p>
---	---	--

at the Met Office and at DWD, respectively, are described in more detail in the evaluation report of ATMS/NOAA-20 data (see Harlow et al., 2019, sections 3.1.1 and 3.2). AMSU-A and MHS carry similar frequencies to ATMS and the data screening of both instruments is handled in the same way. At DWD, also data over sea-ice and land are excluded for the lower peaking channels AMSU-A 1-8 based on digital land data as well as detection using AMSU-A observations.

At DWD, the same data screening is done for AMSU-A and MHS on Metop-A, -B, and -C. At the MetOffice, Metop-C data have a different mapping (see above), but channel selection is not affected by a cloud detection test which utilizes HIRS. Apart from these two differences the pre-processing and quality control is also the same as for the other Metop platforms.

An initial assessment by EUMETSAT on the instrument's performance post launch concluded that the AMSU-A instrument was performing as expected, but noted increased noise and striping on MHS channels 3 and 4. The poorer performance of the MHS channels is highlighted in Figure 1, which shows estimated instrument noise for several orbits of data from the three MHS instruments on the Metop satellites.


At the Met Office, three months of passive monitoring of Metop-C AMSU-A and MHS data was performed during winter 2018/19. The first month of data was used to calculate O-B statistics split into latitude bands, which are used to compute static bias correction coefficients. The coefficients were then held fixed and used to correct the observations made during the latter two months of passive monitoring. The following plots referred to in this section present differences between the bias corrected observations and the operational global NWP model (OS41 configuration), hereafter referred to as C-B.

Figure 2 shows a summary of the C-B differences expressed as a standard deviation for each channel, and all three satellites. Results for Metop-C are very encouraging and comparable to the other platforms, with the exception of MHS channels 3 and 4, where the larger instrument noise is reflected in increased C-B standard deviations (~2 K for Metop-C versus ~1.5 K for Metop-A and -B). As an example of the encouraging performance, AMSU-A channel 6 is a key channel in our assimilation scheme and the C-B standard deviation values for this channel on Metop-A, -B and -C are found to be 0.12, 0.14, 0.13 K respectively.

Figure 3 shows a time series of C-B statistics for key temperature sounding channels on Metop-C. Results appear very stable with the exception of short periods of increased noise for channels 7 and 8, on the 11th December 2018 and 17th January 2019 respectively. EUMETSAT has also reported sporadic noise in AMSU-A channel 3. This is not apparent from our monitoring, either in clear or cloud conditions over sea. At the Met Office the effect of this noise increase is unlikely to pose an issue for the use of this channel in assimilation because the observation error assumed in 4D-Var for channel 3 is currently 2 K due to increased surface emission for this low opacity channel.

At DWD, the data have been evaluated for a similar initial period, between the beginning of December 2018 and early February 2019 in a passive mode (i.e. not assimilated) and compared to the already actively assimilated Metop-A and -B data. The bias correction (versus FG fields) applied is an online scheme, where the mean correction and air mass dependent bias correction predictor coefficients are continuously updated after each assimilation cycle to account for variations of bias in time. The bias correction reaches a relatively stable state after the accumulation of sufficient statistics which is typically after a few days for AMSU-A and MHS data.

Figure 4 shows results for all AMSU-A channels for the two months 6 December 2018 to 7 February 2019 for the passive Metop-C data in comparison to the actively assimilated Metop-A and -B data (top panel), The standard deviations of the bias corrected OBS-FG departures (corresponding to C-B in Met Office plots) show that AMSU-A on Metop-C has similar or smaller values than Metop-A and -B, with the exception of channels 5, 6 and 8 where values are slightly larger. Figure 5 displays the standard deviations OBS-FG for

 <p>EUMETSAT NWP SAF NUMERICAL WEATHER PREDICTION</p>	<p>Report on MetOp-C AMSU-A, MHS and IASI radiance data quality.</p>	<p>Doc ID : NWPSAF-MO-TR-037 Version : 1.3 Date : 17/02/2020</p>
---	---	--

these three channels as time series over the two months for Metop-C in comparison to Metop-B values. The larger standard deviations can be seen particularly at the start of the period but are getting smaller from about mid January 2019 onwards. Towards the end of the period, values of Metop-C are comparable to Metop-B for channels 5 and 8 and even smaller for channel 6. To cross-check, the comparison between all three satellites has been added for a second more recent period between 11 October and 5 December 2019 in Figure 4(b). This confirms that AMSU-A on Metop-C has comparable to slightly better quality than the instruments on Metop-A and –B. Overall standard deviation values are a little smaller for several channels in the later period. This is probably also reflecting small improvements in the model FG due to several operational upgrades (e.g. also the introduction of Metop-C data from AMSU-A, MHS, radio occultation, scatterometer and AMVs).

Figure 6 shows similar statistics for MHS channels 1-5. As in the evaluation at the Met Office, also the DWD comparison versus ICON/DWD shows clearly the lower quality of the channels 3 and 4 on Metop-C with standard deviations being about 0.2 K and 0.3 K larger, respectively. Figure 7 shows mean biases of uncorrected OBS versus FG values as a function of scan position across the swath for AMSU-A channels 5 to 14 and MHS channels 3 to 5 for Metop-B and Metop-C instruments. Results for both satellites are similar in that the channels generally have similar characteristics across the scan, but absolute values between both satellites may vary. A bias variation of OBS-FG across the scan can be caused either by the observations themselves, but also model biases varying with height can contribute (as the height of the sensed layer increases due an upwards shift of the weighting function with increasing scan angle). Scan dependent biases versus the model FG are corrected as part of the applied bias correction procedure.

Overall, the results of both the Met Office and DWD are consistent and show that AMSU-A on Metop-C has a similar to slightly better quality than AMSU-A on Metop-A and –B, while MHS on Metop-C channels 3 and 4 are noisier and channel 5 is again of the same quality.

2.3. IASI instrument characteristic and data processing


IASI is a Fourier transform spectrometer based on the Michelson interferometer which was developed by the Centre National d'Etudes Spatiales (CNES) in cooperation with EUMETSAT (Siméoni et al., 1997). IASI has a horizontal resolution of 12 km and a swath width of 2200 km which gives almost global coverage in one day. It measures between 645 cm^{-1} and 2760 cm^{-1} at 0.25 cm^{-1} intervals and 0.5 cm^{-1} spectral resolution and has sensitivity to atmospheric temperature, humidity and clouds as well as a number of trace gases and aerosols. Channels selected for assimilation, and this evaluation study, at the Met Office and at DWD typically focus on the temperature and humidity signals, but exclude trace gas sensitivities. At the Met Office Level 0 data from IASI are received locally and processed to calibrated radiances using the AAPP package (Atkinson, 2017). Global data are received via the EUMETCast service.

Figure 8 shows the channel selection used by the Met Office, with 175 channels used in the pre-processing and a subset of 130 channels used in the variational assimilation system (VAR). The channels have been selected based on the initial 314 channels recommended for NWP systems by Collard (2007) and subsequent NWP forecast impact trials. Of the 130 channels used 107 are from band 1 (645 to 1210 cm^{-1}) and 23 are from band 2 (1210 to 2000 cm^{-1})

At DWD, the global data received through EUMETCast are used. From the full 8641 channel data set, the standard 354 channel subset (corresponding to the updated channel set recommended for NWP systems) is extracted for ingest and monitoring. The pre-processing checks L1 processing flags in the data and for unphysical values.

2.4. IASI Monitoring results

To check the quality of the IASI instrument on Metop-C, observed brightness temperatures (O) have been compared against simulated brightness temperatures from short-range forecast fields, in a similar manner as

 <p>EUMETSAT NWP SAF NUMERICAL WEATHER PREDICTION</p>	<p>Report on MetOp-C AMSU-A, MHS and IASI radiance data quality.</p>	<p>Doc ID : NWPSAF-MO-TR-037 Version : 1.3 Date : 17/02/2020</p>
---	---	--


the microwave instruments previously discussed. Statistics are computed using data free from major sources of uncertainty, such as inaccurate surface emission values and cloud. The data selection at the Met Office includes data quality controlled for convergence of a 1D-var scheme. The 1D-var scheme retrieves the cloud amount and cloud top height in a profile. The cloud information is used to remove channels from the variational system which have significant sensitivity below the cloud top height. The channel selection used for the pre-processor and the variational system are shown in Figure 8. At DWD, a cloud screening is done using the McNally & Watts scheme (McNally and Watts, 2006) and the current evaluation is limited to data over sea and excludes outliers using a standard FG-check. Results from the Met Office evaluation are displayed in Figure 9 showing the mean and standard deviation of the O-B's for the 175 channels used in the pre-processing for IASI on Metop-A, -B and -C. The data are after quality control but before thinning and cases for cloud-affected scenes are likely to be included here but grossly erroneous data have been removed by the 1D-var pre-processing. The mean biases for Metop-C IASI are comparable with the other IASI instruments. In the window region around 900 cm^{-1} the biases are slightly more positive than the other instruments. The standard deviation of the uncorrected O-B is comparable with Metop-A and -B and perhaps a little smaller in the CO_2 temperature sounding channels.

In order to calculate corrected brightness temperatures (C, observations plus a bias correction term), initial bias correction values were derived from two weeks of monitoring. The bias correction increments were then held static for May 2019 to calculate the innovation statistics. Figure 10 shows the mean and standard deviation C-B statistics for May 2019 for the 30 channels used in the variational assimilation system. The C-B values show the observations can be corrected to similar values to the other IASI instruments. There is a slight negative offset for Metop-C compared with Metop-A and -B which is the result of the bias correction coefficients. There are 9 channels out of the 130 channels which have a static bias correction around 900 cm^{-1} which is producing a slightly better fit throughout the spectrum for Metop-C relative to Metop-A and -B. This could be because these have been newly calculated for Metop-C and the Metop-A and -B coefficients may need updating or just be a function of the time period studied. The standard deviation of C-B for Metop-C a little smaller than for Metop-A and -B for all channels.

Corresponding results for standard deviation of the bias corrected OBS-FG from the DWD monitoring are shown in Figure 11 for the 354 channel set covering the spectrum from $\sim 650\text{ cm}^{-1}$ to $\sim 2200\text{ cm}^{-1}$. Of all the three IASIs, the one on Metop-C shows the best performance, especially at the longwave edge of the spectrum (below 900 cm^{-1}) as is visible from the lower panel showing the relative difference of standard deviations versus the IASI instrument on Metop-A. The results of both the Met Office and DWD confirm the excellent quality of this last IASI of the series and indicates it is performing even a little better than IASI on Metop-A and -B.

Figure 12 shows a timeseries of corrected innovations (C-B) for a selection of channels based on the Met Office evaluation results. The bottom plot of Figure 12 shows the observation count used in VAR for a high peaking temperature sounding channel for the three Metop instruments. The periods with no observations are data outages for Metop-C IASI on the 14-15 and the last few days of May. The channels at 657.5 cm^{-1} and 726.5 cm^{-1} are high and low peaking temperature sounding channels respectively (temperature jacobian peak at 50 hPa and 792 hPa, respectively). Both of these temperature sounding channels have been corrected to very small innovations for all three Metop satellites with the performance of Metop-C being comparable with the other platforms. The channel at 901.5 cm^{-1} is a window channel with the data being corrected to less than 0.2 K with the innovation slightly smaller for MetopC for this period. The channel at 1367 cm^{-1} is a mid peaking water vapour channel (temperature jacobian peak at 638 hPa). The innovation of the water vapour channel for MetopC is slightly more negative than the other IASI's but about the same magnitude and within the error assumed in the assimilation. The stability of the timeseries data shows that the instrument is performing as expected. In the operational system there are 9 channels in the window region around 900 cm^{-1} which have a fixed bias correction, the remaining channels are all corrected by variational bias correction (VarBC).

Figure 13 shows the spatial coverage for a six hour assimilation cycle at the Met Office with (bottom) and without (top) Metop-C. This shows that the amount of data and spatial coverage is only slightly increased

 <p>EUMETSAT NWP SAF NUMERICAL WEATHER PREDICTION</p>	<p>Report on MetOp-C AMSU-A, MHS and IASI radiance data quality.</p>	<p>Doc ID : NWPSAF-MO-TR-037 Version : 1.3 Date : 17/02/2020</p>
--	---	--

with the additional of the third satellite. There is an increase of around 10 % in the total number of IASI observations that are passed to the variational system after thinning. The inclusion of an additional satellite should improve redundancy and the continuation of the Metop mission when Metop-A reaches its end of life in 2022.

3. Data Timeliness

Figure 14 and 15 illustrate the timeliness of data reception for Metop-C in comparison to Metop-A and -B. Timeliness is defined as the difference between the observation time and the storage time in the data bank and thus comprises the time needed for L1b data processing (on-board and in the ground system), the transmission time (downlink from the satellite and transmission via EUMETCast) as well as some (small) additional time between reception at the weather service and data bank entry. Data coverage and timeliness are monitored by both the Met Office and DWD for the NWP-SAF (see <https://www.nwpsaf.eu/site/monitoring/nrt-availability/data-timeliness/>)

Figure 14 shows the timeliness for AMSU-A and MHS for all three Metop satellites for the month of October 2019 from the DWD timeliness monitoring. The timeliness is very stable and also consistent between the DWD and the Met Office with only very small differences (of the order of a few minutes). All data from the global reception arrive well within 1-2 hours after the observation. Metop-C has very similar timeliness to Metop-A with approximately 90 % of the data received in 1.5 hours from a single global downlink once per orbit at Svalbard. The data are less timely than Metop-B data (typically 90 % of data in 50 minutes). This is because Metop-B is designated the prime Metop satellite and is thus benefits from a twice orbital data dump over both Svalbard and McMurdo.


Figure 15 shows, in the top panels, similar plots for IASI data comparing Metop-C to Metop-B timeliness, where naturally the same downlink effect is seen that Metop-B data transmission is faster. At the bottom the figure shows a timeseries of the reception delays which illustrates that for both satellites the reception is very stable in time. Occasionally, some data may be slightly delayed (as visible here in the middle pane for Metop-C data), but this is relatively rare.

Additionally, the DBNet service offers a fast transmission for part of the globe using local reception stations and data processing with a retransmission via the EUMETCast service and Metop-C data are included in this service. Figure 16 illustrates the coverage for AMSU-A data and the excellent timeliness of DBNet data with about 90 % of the AMSU-A data normally received within 30 minutes of the observation time. DBNet timeliness for MHS and IASI data are similar. Here, Metop-A -B, and -C data are received and transmitted in a similar way.

4. Conclusions


The quality of the Metop-C AMSU-A, MHS and IASI instruments has been assessed against simulated observations from background model fields and compared against equivalent instruments on Metop-A and -B. These comparisons have been performed using the modelling systems of the Met Office and DWD in order to account for uncertainty in the NWP model fields. In general, the results of both centres are very consistent and show that the characteristics of each of the instruments on Metop-C is comparable with the equivalent instrument on Metop-A and -B.

The AMSU-A and MHS instruments have good performance in terms of the observation departures with respect to the global NWP model. The Metop-C microwave data can be corrected to values which are equivalent to the instruments on Metop-A and -B which are currently used operationally at both the Met Office and DWD. The known issues of increased noise on MHS channels 3 and 4 are clearly visible in the NWP comparisons as well as very short bursts of increased noise on AMSUA channels 7 and 8.

 <p>EUMETSAT NWP SAF NUMERICAL WEATHER PREDICTION</p>	<p>Report on MetOp-C AMSU-A, MHS and IASI radiance data quality.</p>	<p>Doc ID : NWPSAF-MO-TR-037 Version : 1.3 Date : 17/02/2020</p>
--	---	--


The NWP monitoring also confirms the excellent quality of the Metop-C IASI instrument. Observation departures from the model background have standard deviations which are slightly smaller than Metop-A and -B, especially at the longwave edge of the spectrum. The data can also be corrected to an equivalent low bias. The timeseries data show the observations have good stability and a similar number of observations pass quality control checks as is seen for Metop-A and -B.

The timeliness of the AMSU-A, MHS and IASI data for Metop-C is similar to that of Metop-A (within about 1 hour and 50 minutes for the global data sets), but not as good as the timeliness of Metop-B data which continues to be the prime EPS satellite benefitting from two downlinks per orbit. The locally received and retransmitted DBNet data of Metop-C reach the same very good timeliness arriving mostly within 30 minutes of observation time. Data timeliness and transmission is very stable and reliable.

 <p>EUMETSAT NWP SAF NUMERICAL WEATHER PREDICTION</p>	<p>Report on MetOp-C AMSU-A, MHS and IASI radiance data quality.</p>	<p>Doc ID : NWPSAF-MO-TR-037 Version : 1.3 Date : 17/02/2020</p>
---	--	--

5. References

- Atkinson N., 2017, AAPP Overview, https://www.nwpsaf.eu/site/download/documentation/aapp/NWPSAF-MO-UD-004_Overview_v8.0.pdf, (accessed 22 January 2019).
- Bootton A., Bell W., Atkinson N., 2014, An improved bias correction for SSMIS, *Proceedings of the 19th International TOVS Study Group conference*, Available from https://cimss.ssec.wisc.edu/itwg/itsc/itsc19/program/papers/10_03_bootton.pdf
- Cameron J. R. N., Collard A. D., English S. J., 2005, Operational use of AIRS observations at the Met Office, Proceedings of ITSC-XIV, Beijing, China, 25 – 31 May 2005. Available from <http://cimss.ssec.wisc.edu/itwg/itsc/itsc14>.
- Chahine, M. T., Pagano, T. S., Aumann, H. H., Atlas, R., Barnet, C., Blaisdell, J., et al. (2006). AIRS: Improving weather forecasting and providing new data on greenhouse gases. *Bulletin of the American Meteorological Society*, 87(7), 911–926. <https://doi.org/10.1175/BAMS-87-7-911>
- Collard, A. D., 2007, Selection of IASI channels for use in numerical weather prediction, *Q. J. R. Meteorol. Soc.*, 133
- Derber J. C. and Wu W.-S., 1998, The use of TOVS cloud-cleared radiances in the NCEP SSI analysis system, *Mon. Weath. Rev.*, 126, 2287–2299.
- English S. J., Renshaw R. J., Dibben P. C., Smith A. J., Rayer P. J., Poulsen C., Saunders F. W., and Eyre J. R., 2000, A comparison of the impact of TOVS and ATOVS satellite sounding data on the accuracy of numerical weather forecasts. *IEEE Trans. Geosci. Remote Sens.*, 46, 403–408.
- Hilton F., Atkinson N. C., English S. J. and Eyre J. R., 2009, Assimilation of IASI at the Met Office and assessment of its impact through observing system experiments, *Q. J. R. Meteorol. Soc.*, 135: 495–505.
- Köpken, 2004: Solar Stray Light Effects in Meteosat Radiances Observed and Quantified Using Operational Data Monitoring at ECMWF. *J. Appl. Met. Clim.*, **43**(1), 28-37.
- Joo, S., Eyre J., Marriott R., 2012, The impact of Metop and other satellite data within the Met Office global NWP system using an adjoint-based sensitivity method. *Met Office Forecasting R&D Technical Report No. 562*. February 2012.
- McNally, T., Watts, P. D., 2006: A cloud detection algorithm for high-spectral-resolution infrared sounders. *Q. J. Roy. Met. Soc.*, 129, 3411-3423
- Migliorini, S., Candy, B. (2019). All-sky satellite data assimilation of microwave temperature sounding channels at the Met Office QJRMS doi: 10.1002/qj.3470
- RFI Workshop final report, 2019: Radio Frequency Interference Workshop, 13-14 September 2018, ECMWF, Reading, <https://www.ecmwf.int/en/learning/workshops/radio-frequency-interference-rfi-workshop>, (accessed 22 January 2019).
- Saunders R., Hocking J., Rundle D., Rayer P., Matricardi M., Geer A., Lupu C., Brundel P., Vidot J., 2013, RTTOV-12 science and validation report. NWPSAF-MO-TV-032 v1.1, EUMETSAT NWP-SAF.

 <p>EUMETSAT NWP SAF NUMERICAL WEATHER PREDICTION</p>	<p>Report on MetOp-C AMSU-A, MHS and IASI radiance data quality.</p>	<p>Doc ID : NWPSAF-MO-TR-037 Version : 1.3 Date : 17/02/2020</p>
--	---	--

Saunders R., Hocking J., Turner E., Rayer P., Rundle D., Brunel P., Vidot J., Roquet P., Matricardi M., Geer A., Bormann N., and Lupu C., 2018, An update on the RTTOV fast radiative transfer model (currently at version 12), *Geosci. Model Dev.*, 11, 2717–2737, doi: 10.5194/gmd-11-2717-2018.

Siméoni D., Singer C., Chalon G., 1997, Infrared atmospheric sounding interferometer. *Acta Astronautica*, 40: 113–118.

6. Figures

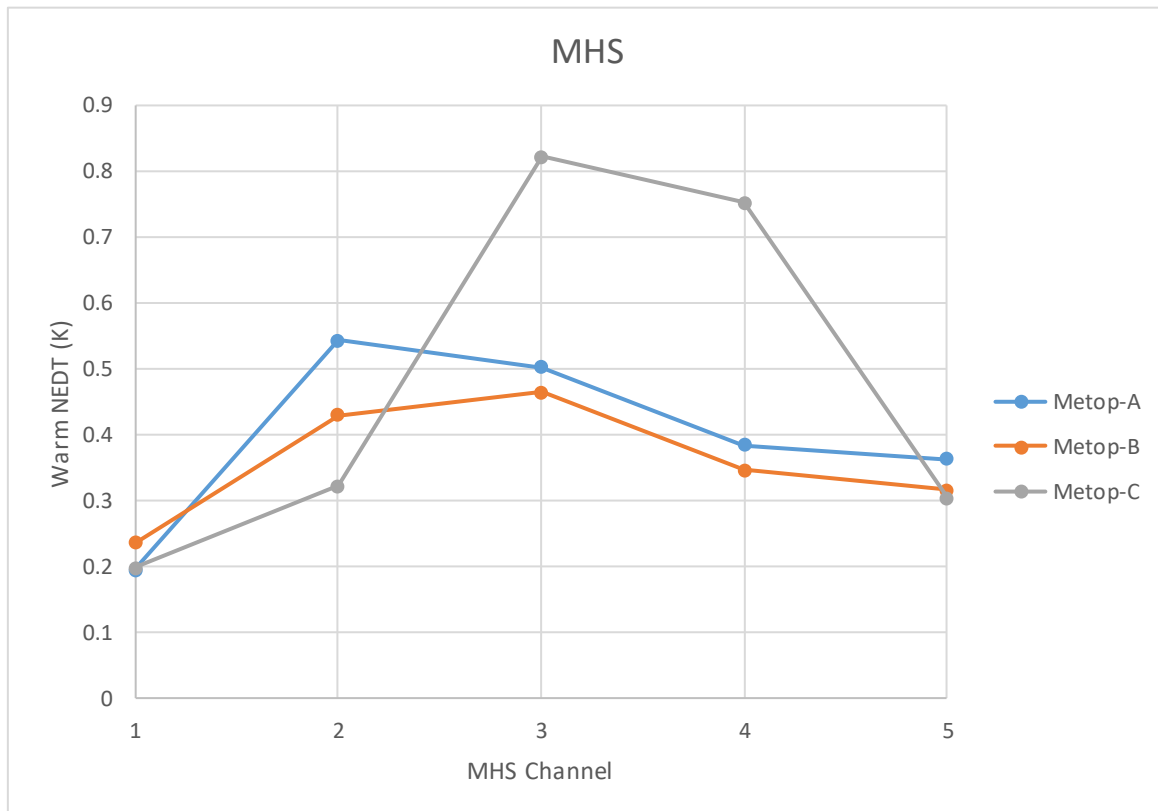


Figure 1: MHS instrument noise averaged over several orbits of data during December 2018.

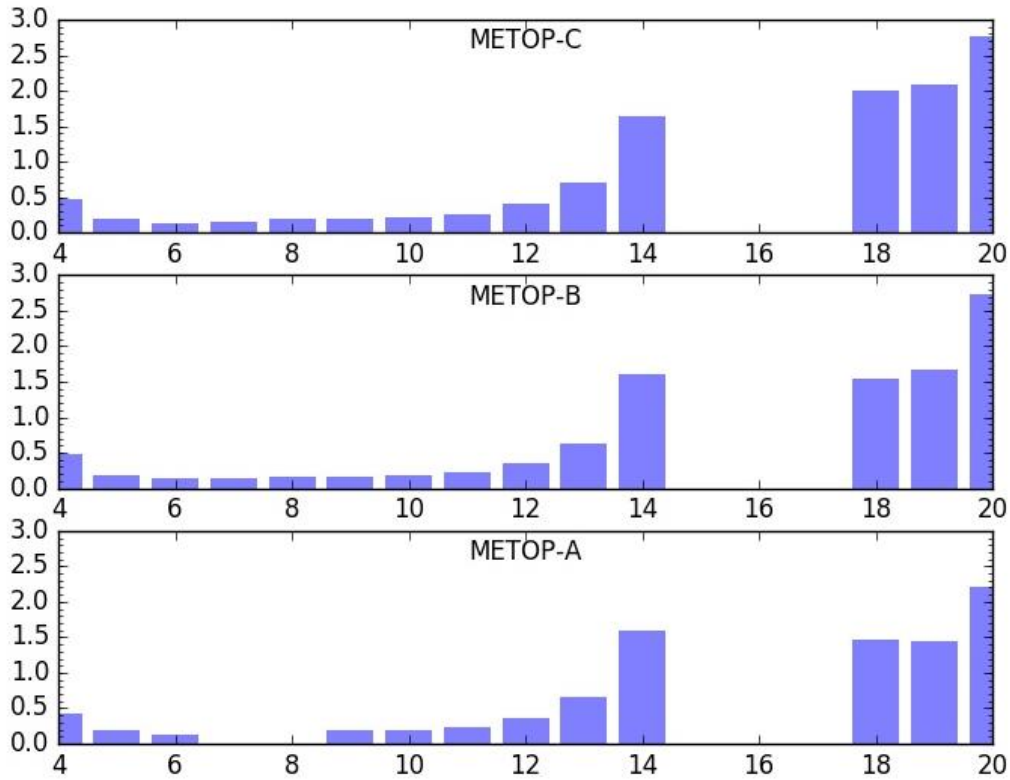


Figure 2: Evaluation results for AMSU-A and MHS versus MetOffice UM first guess: Standard deviation of C-B (K) during winter 2018/19 for AMSU-A and MHS channels on each Metop platform. Channels 4-14 correspond to AMSU-A channels 4-14. Channels 18-20 correspond to MHS channels 3-5. These are the 14 channels which are used in VAR.

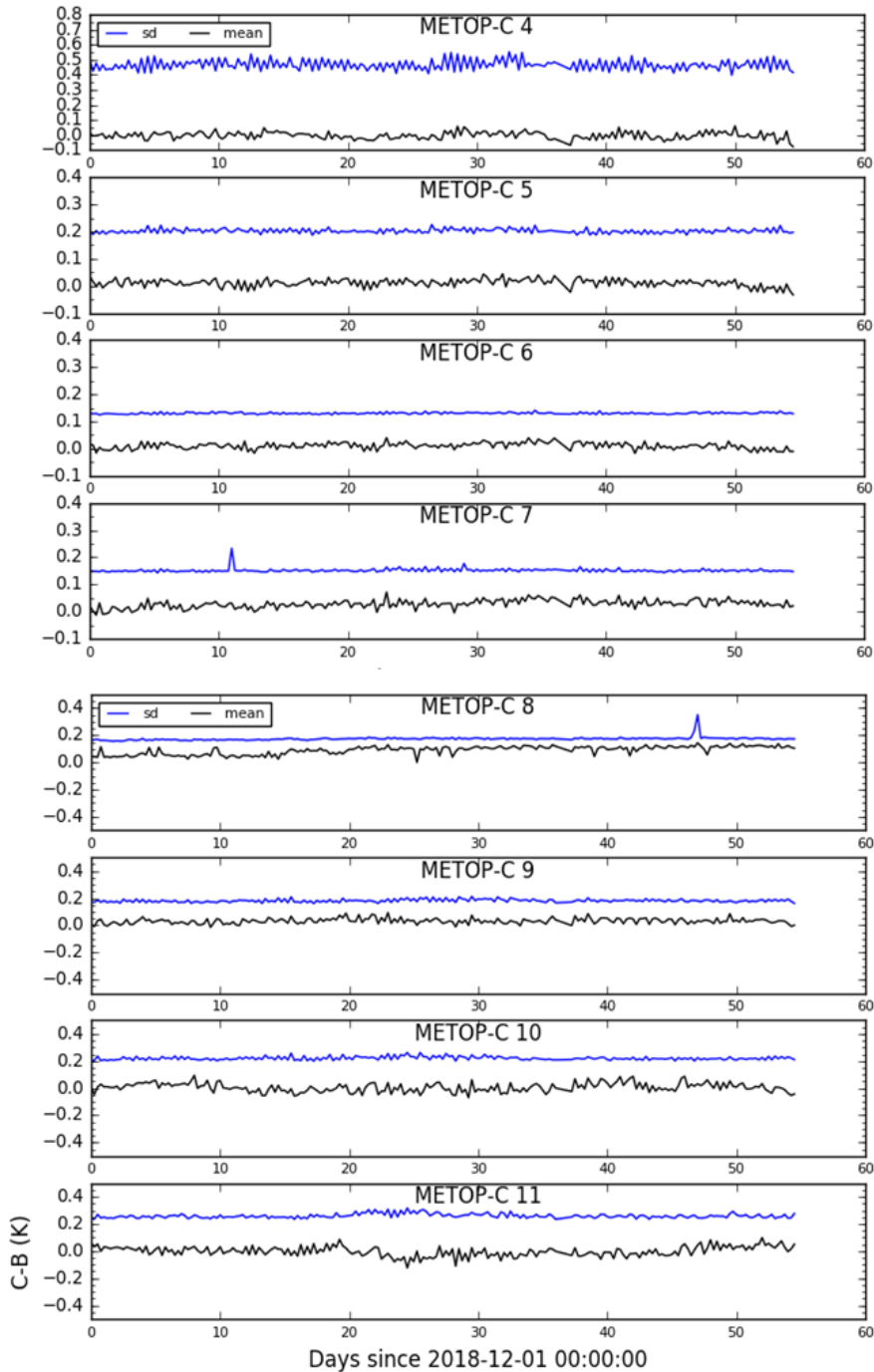


Figure 3: Evaluation results for AMSU-A and MHS versus MetOffice UM first guess: Time series of C-B statistics (K) during winter 2018/19 for key AMSU channels on Metop-C.

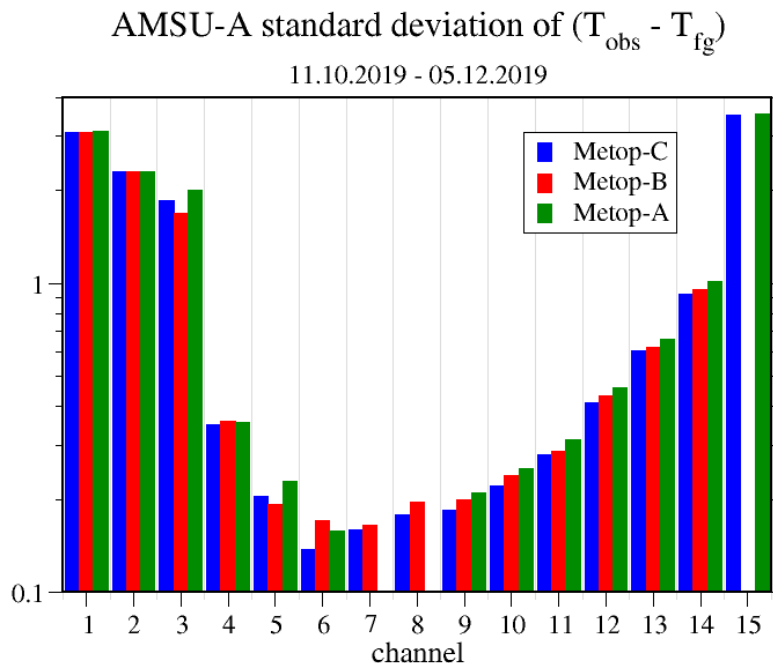
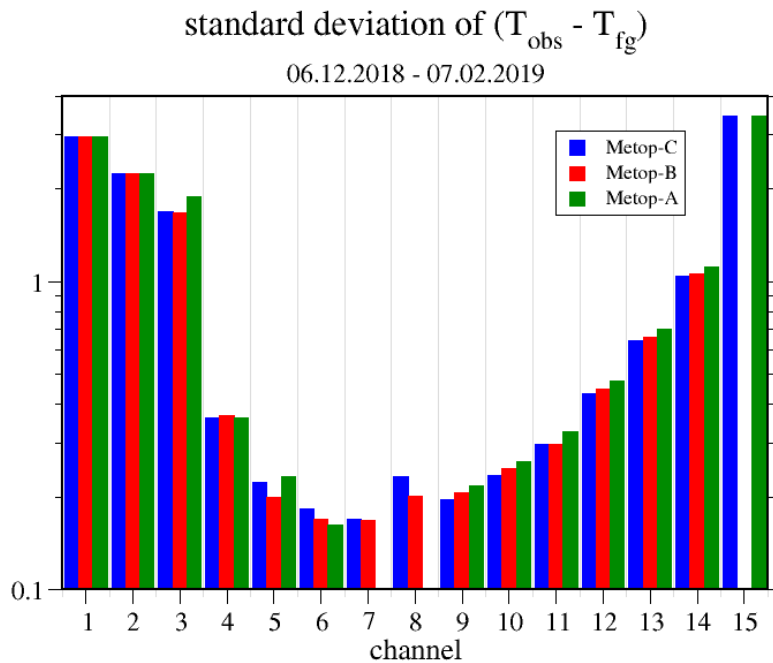


Figure 4: Evaluation results for AMSU-A versus DWD ICON model first guess: Standard deviation of bias corrected OBS-FG (also named C-B) for AMSU-A on Metop-C in comparison to AMSU-A on Metop-A and -B results for a) the period 6.12.2018 to 7.2.2019 shortly after the AMSU-A on Metop-C data became available (top) and b) the recent period 11.10.2019 – 5.12.2019. The y-axis is in logarithmic scaling in [K].

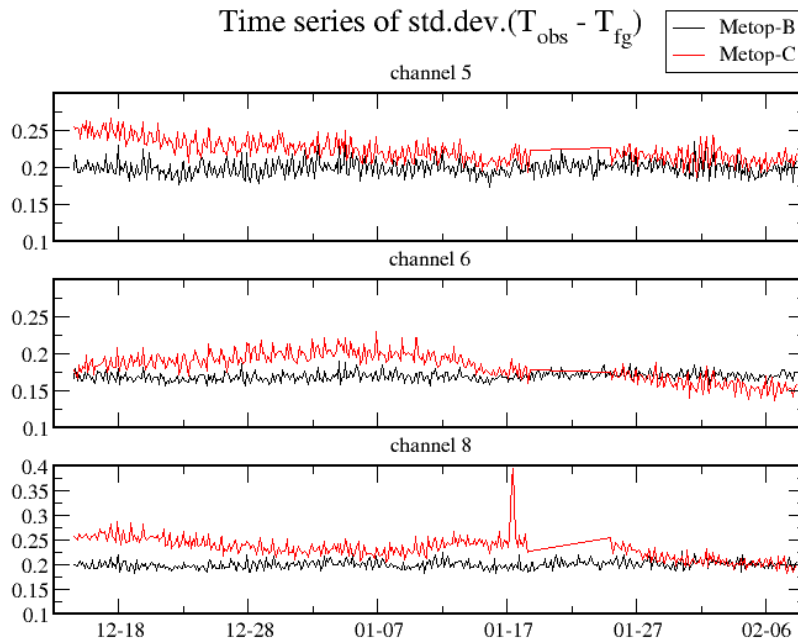


Figure 5: Evaluation results for AMSU-A versus DWD ICON model first guess: Time series of standard deviations of bias corrected OBS-FG (also named C-B) in [K] for AMSU-A for the three channels 5, 6, and 8 comparing Metop-B and -C results for the initial evaluation period 6.12.2018 to 7.2.2019 shortly after the AMSU-A on Metop-C data became available.

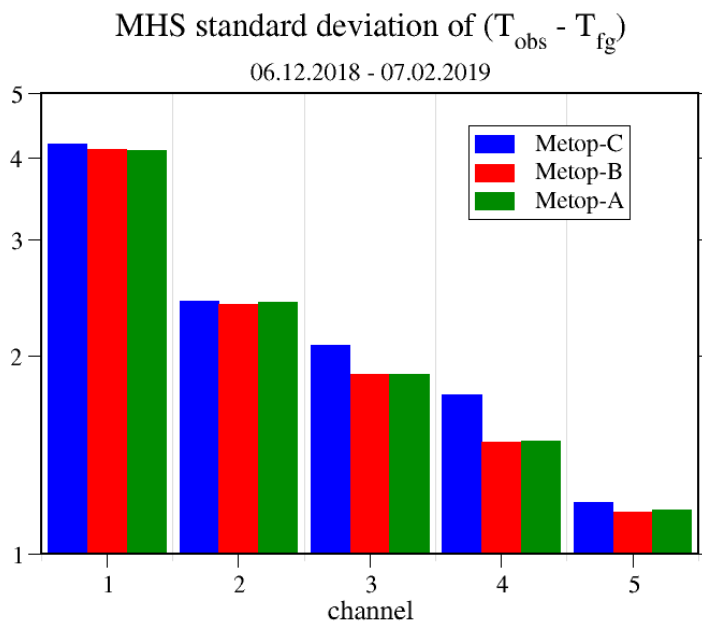


Figure 6: Evaluation results for MHS versus DWD ICON model first guess: Standard deviation of bias corrected OBS-FG (also named C-B) for MHS on Metop-C in comparison to Metop-A and -B results for the period 6.12.2018 to 7.2.2019. The y-axis is in logarithmic scaling in [K].

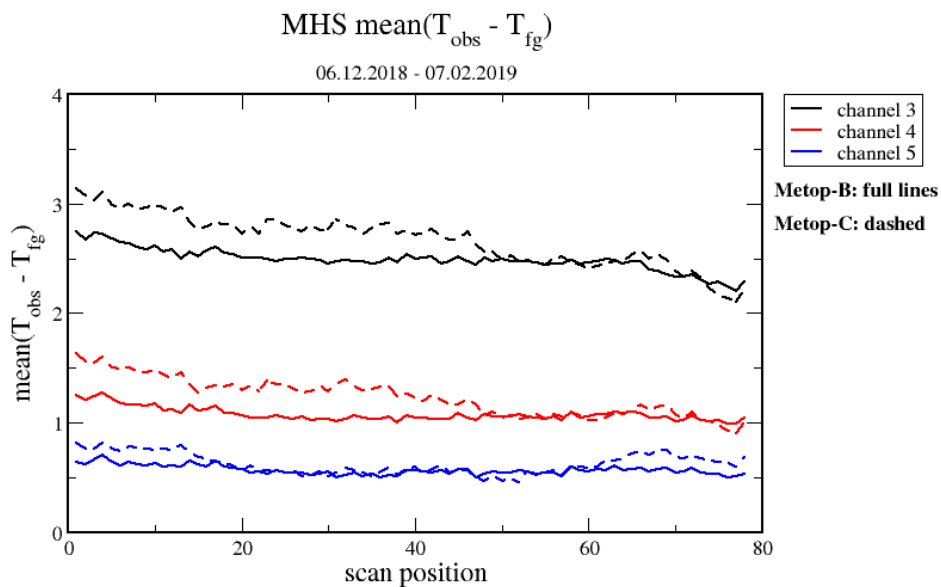
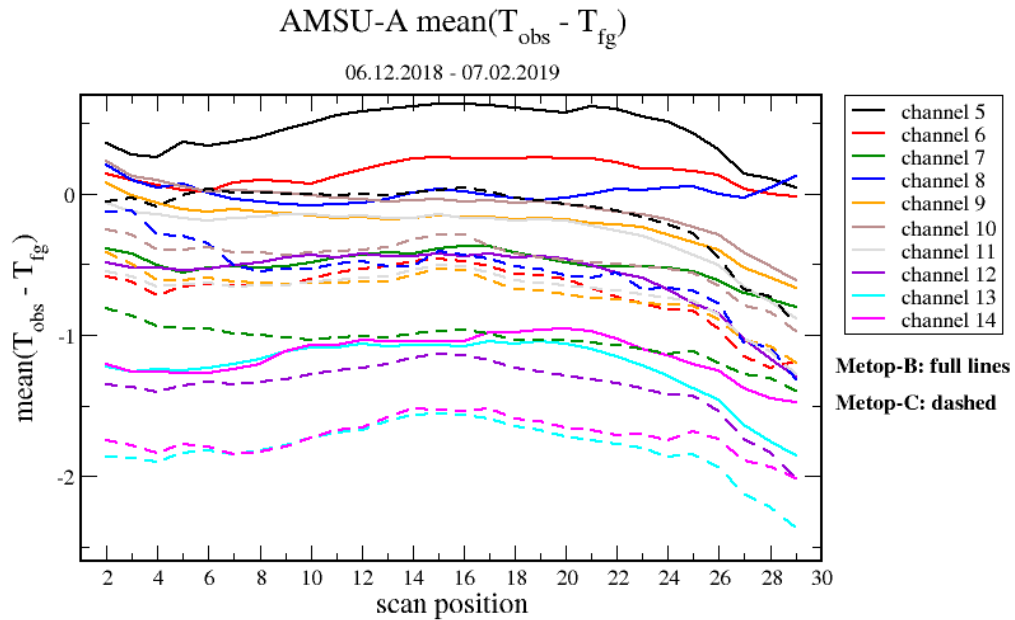


Figure 7: Evaluation results for AMSU-A and MHS on Metop-C versus DWD ICON model first guess: Mean differences of uncorrected OBS-FG brightness temperatures in [K] versus scan position for AMSU-A (top) and MHS (bottom) for the initial evaluation period 6.12.2018 to 7.2.2019. Results for Metop-C (dashed lines) are shown in comparison to Metop-B (solid lines).

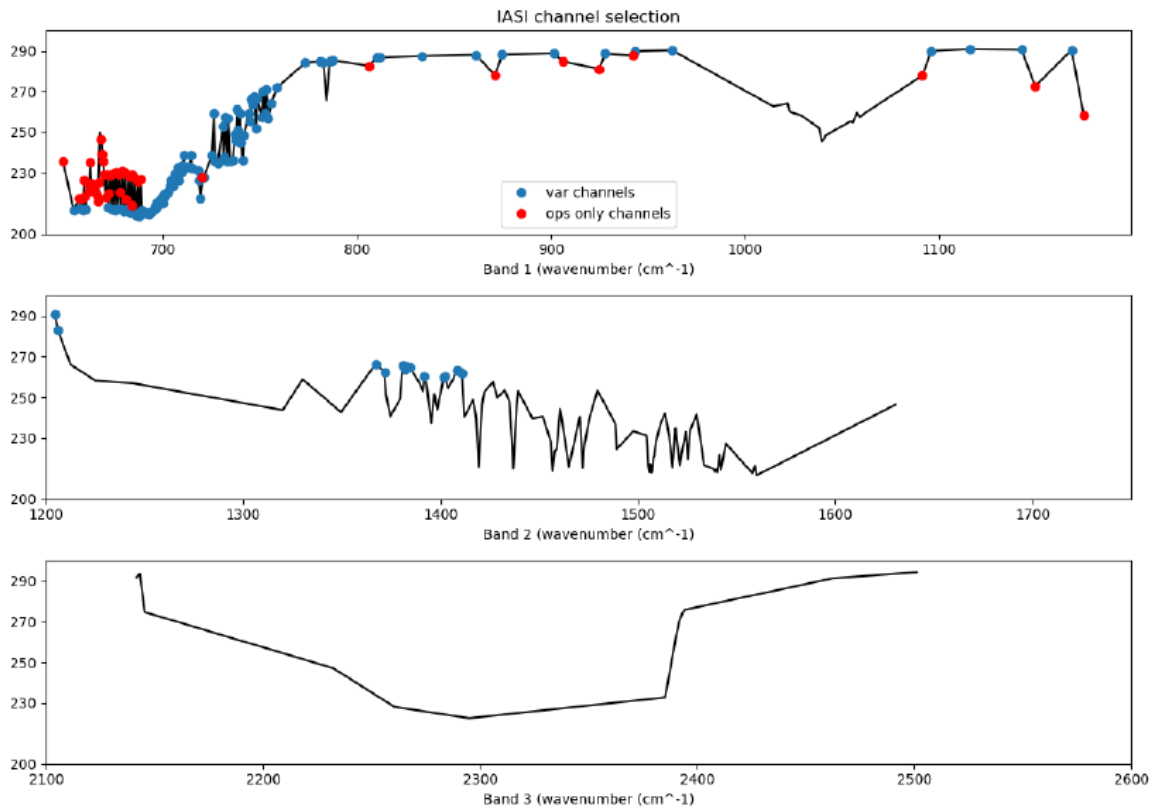


Figure 8: Typical IASI spectrum with channel selection at the Met Office. Channels used only in the pre-processing (OPS) are red. Channels used in the OPS and the variation system (VAR) are shown in blue.

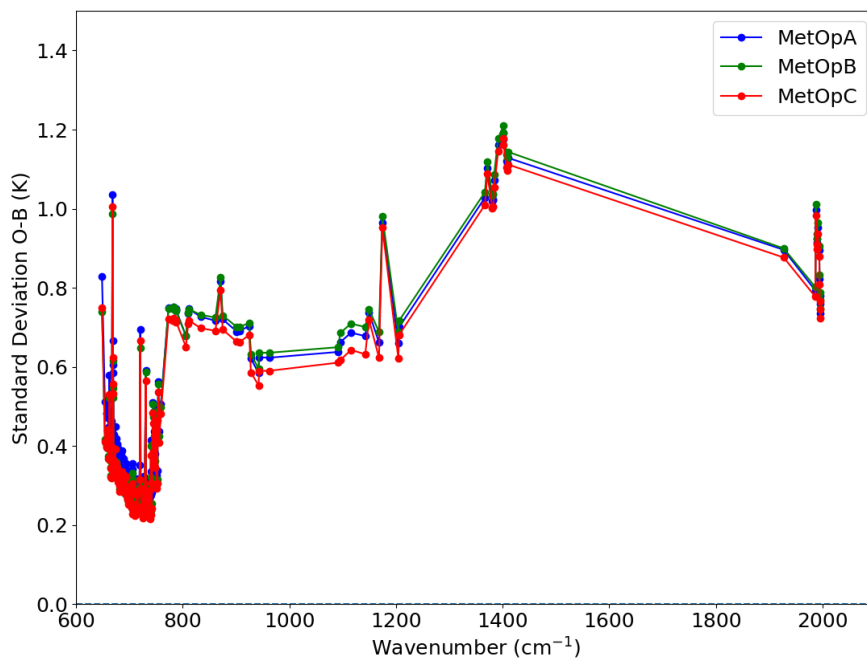
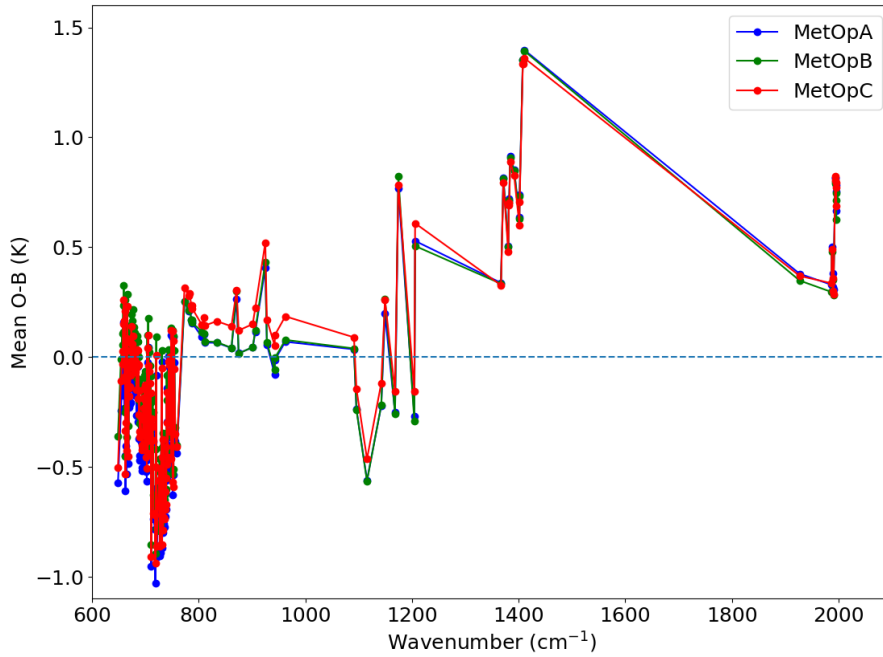


Figure 9: Evaluation results for IASI versus MetOffice UM first guess: Observation minus background mean (a) and standard deviations (b) averaged between 01/05/2019 at 0Z to 31/05/2019 at 18Z for IASI on MetopA, MetopB and MetopC from the Met Office's operational system.

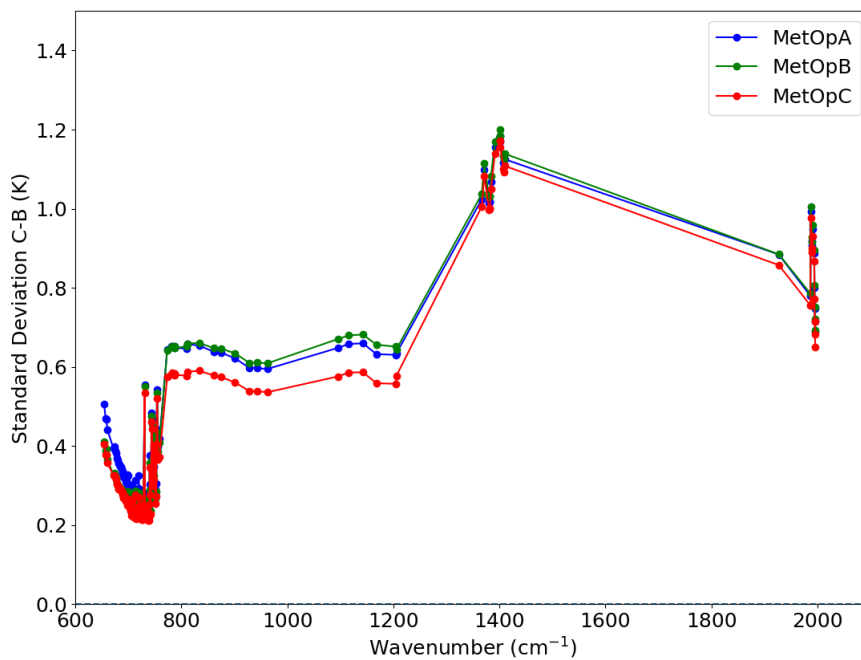
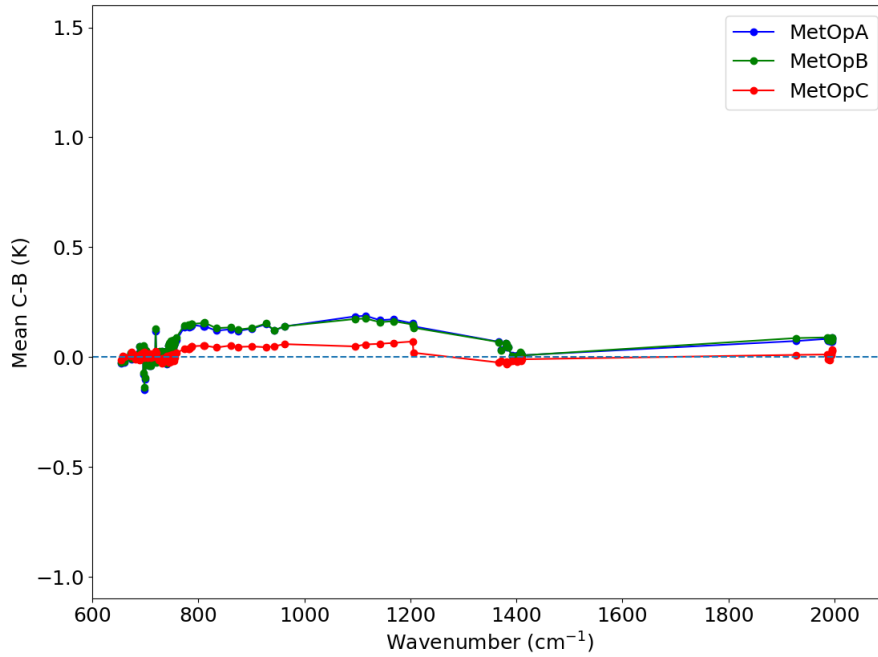


Figure 10: Evaluation results for IASI versus MetOffice UM first guess: Mean and standard deviation C-B statistics for all three IASI instruments for the 130 channels used in VAR from the Met Office's operational system after quality control and before thinning. The data is averaged between 01/05/2019 at 0Z to 31/05/2019 at 18Z.

obs-fg std.dev. (bias corrected)

2019040809-2019051318

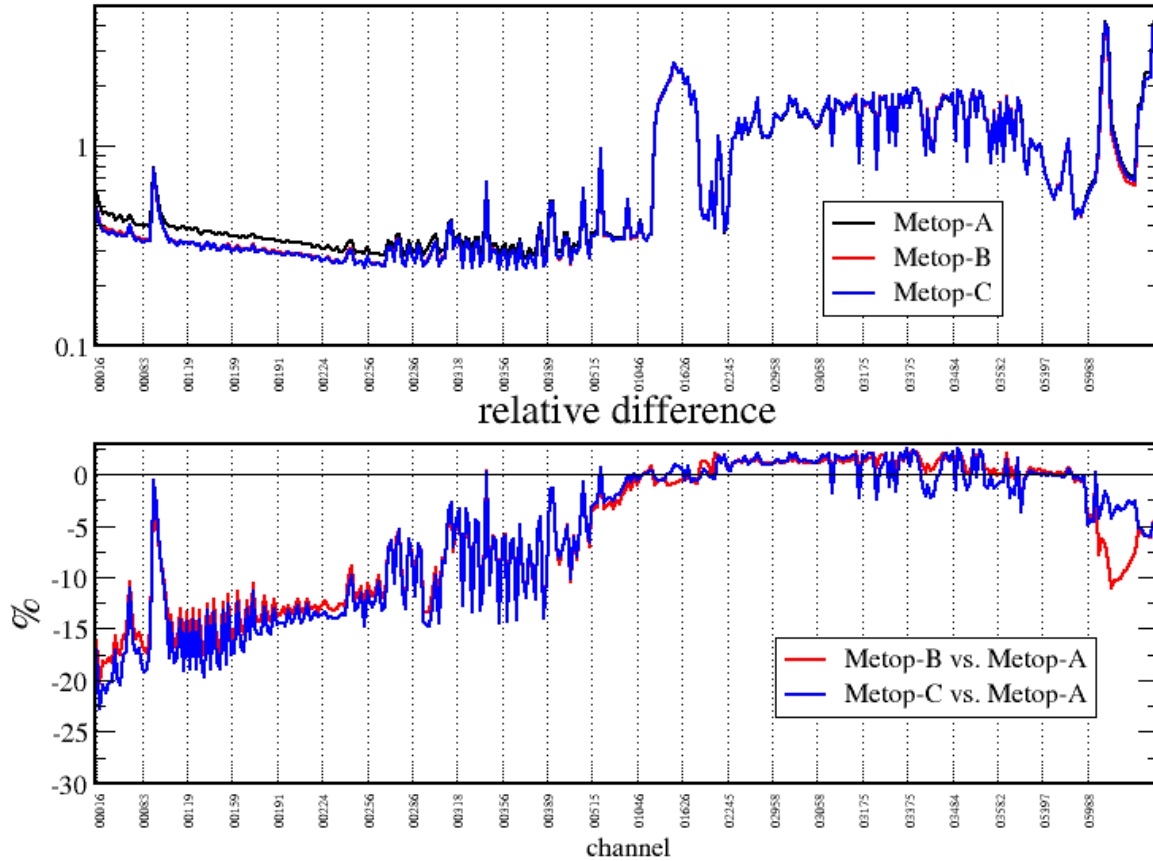


Figure 11: Evaluation results for IASI versus DWD ICON first guess. Top: standard deviation (middle) of bias corrected OBS-FG statistics in [K] for all three IASI instruments after quality control and before thinning; y-axis is logarithmic.. Bottom panel shows the relative difference of standard deviations of IASI on Metop-C and -B compared to IASI on Metop-A. The data is averaged for the period 08/04/2019 at 9 UTC to 13/05/2019 at 18 UTC.

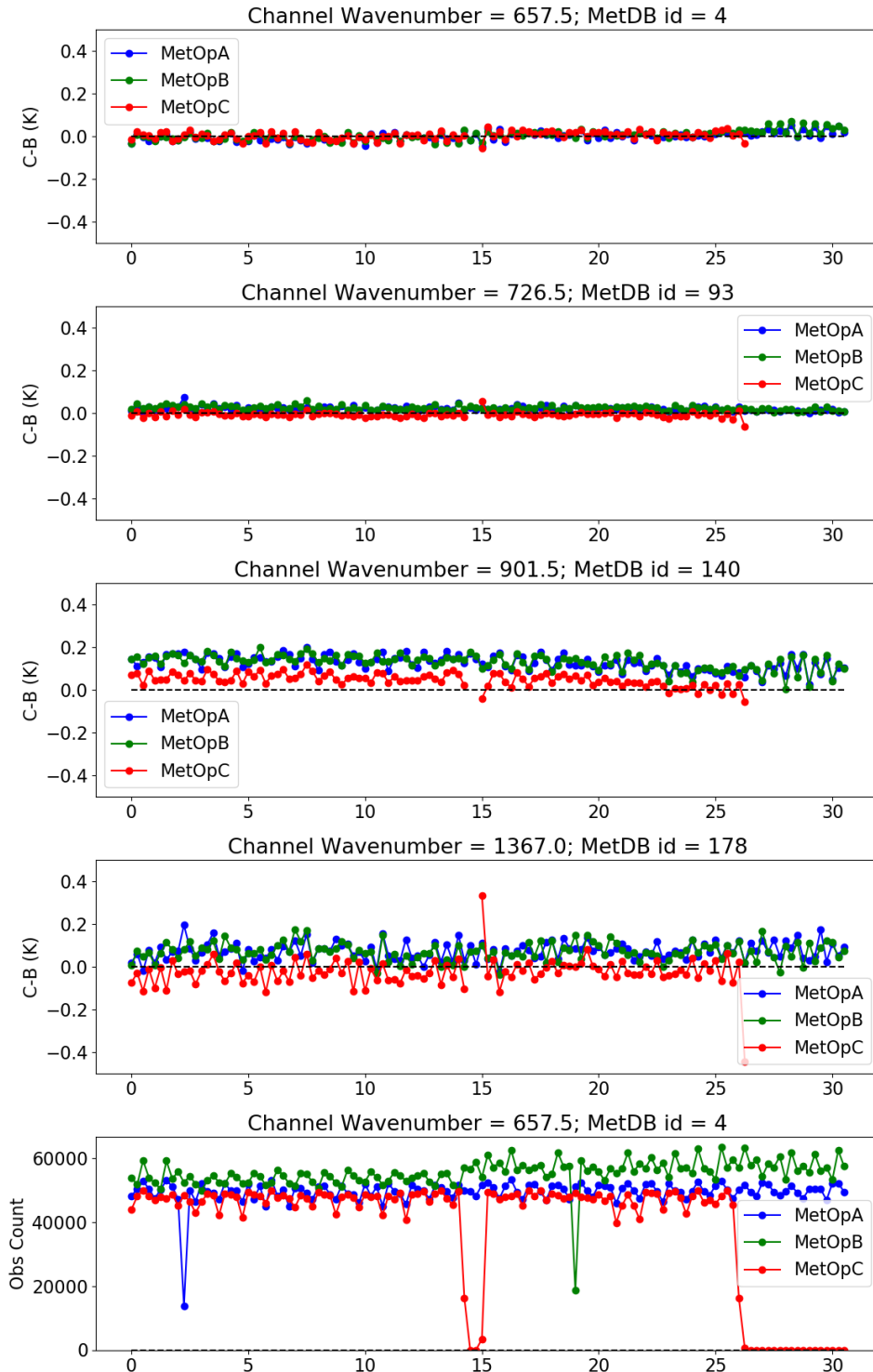


Figure 12: Evaluation results for IASI versus MetOffice UM first guess: Timeseries of corrected innovations from the background for four channels. The observation count for a high peaking temperature sounding channel is shown in the bottom panel. The timeseries is days since 01/05/2019 at 0Z.

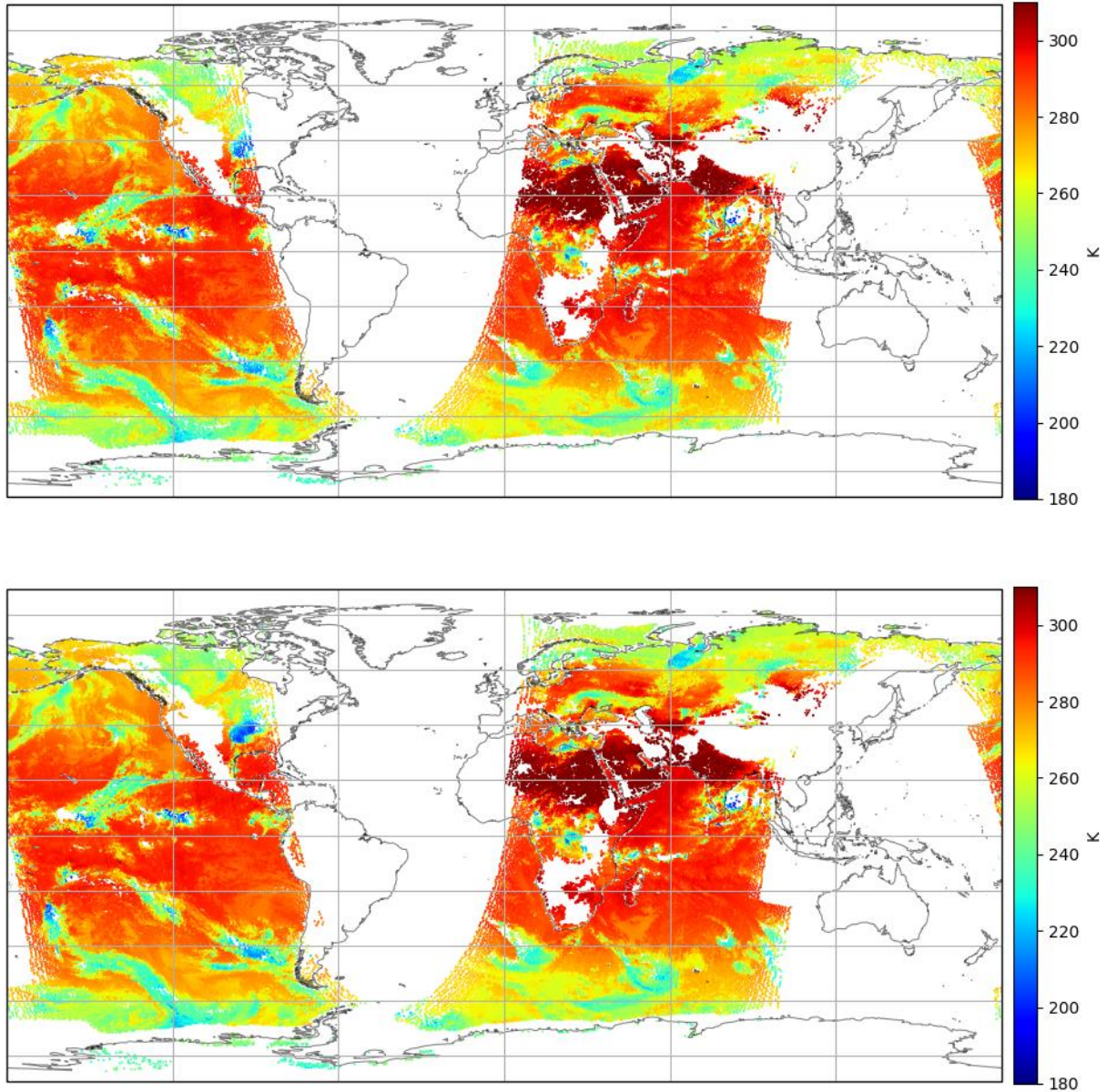


Figure 13: Typical data coverage plot for one six hour assimilation window for just MetopA and MetopB (top plot) and with the addition of MetopC (bottom plot). The plots show the brightness temperature of the window channel at 810.25 cm⁻¹ for the cycle beginning on 01/05/2019 at 6Z.

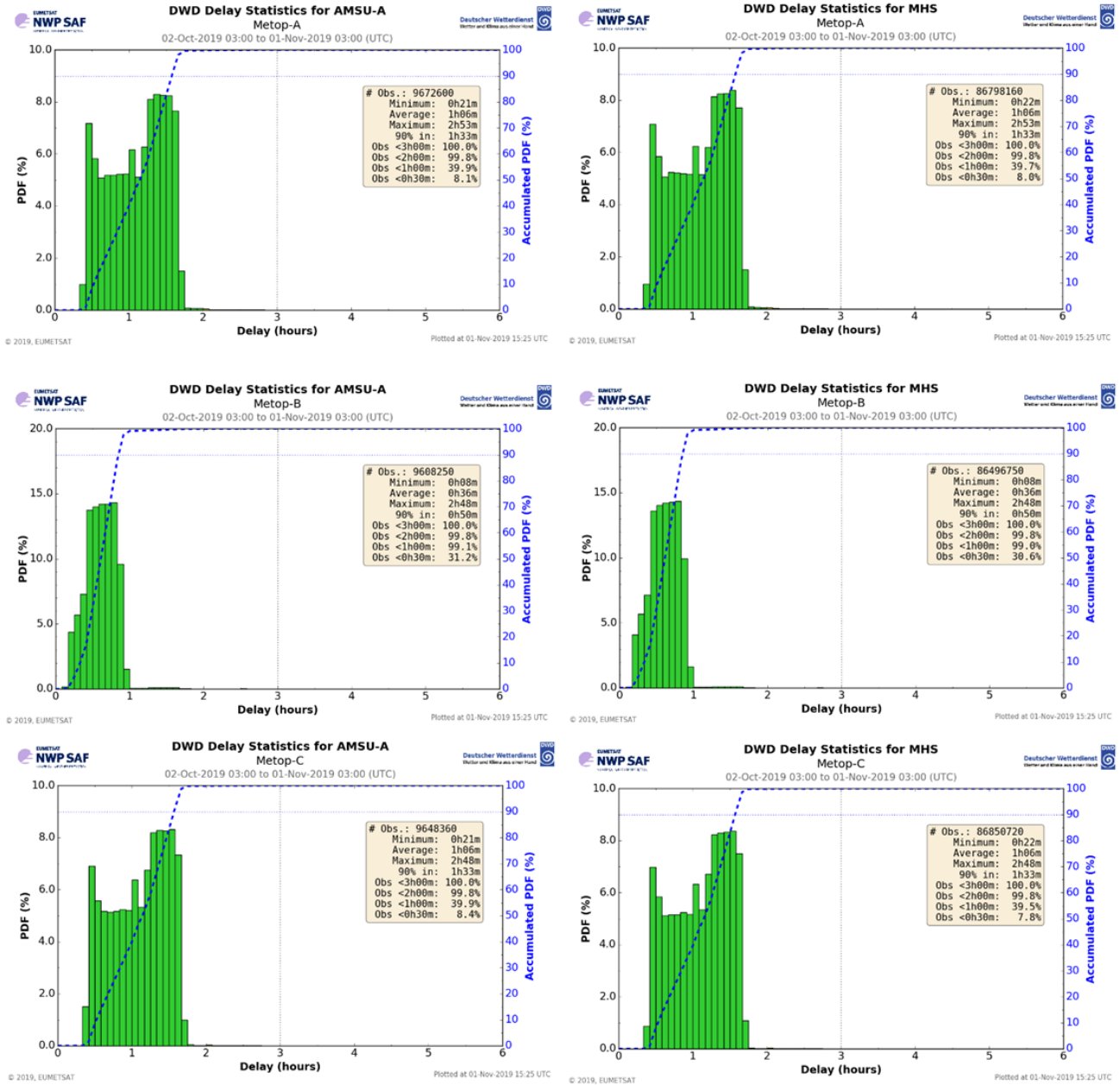


Figure 14: Monitoring of timeliness of AMSU-A L1b data (left) and MHS L1b data (right) from Metop-A (top), Metop-B (middle) and Metop-C (bottom) for the period 2/10/2019-1/11/2019 from the DWD timeliness monitoring. Display is as pdf's of timeliness (defined as elapsed time between observing time and entry time into DWD data base) and accumulated pdf (blue dashed line). Data are received via the EUMETCast transmission service.

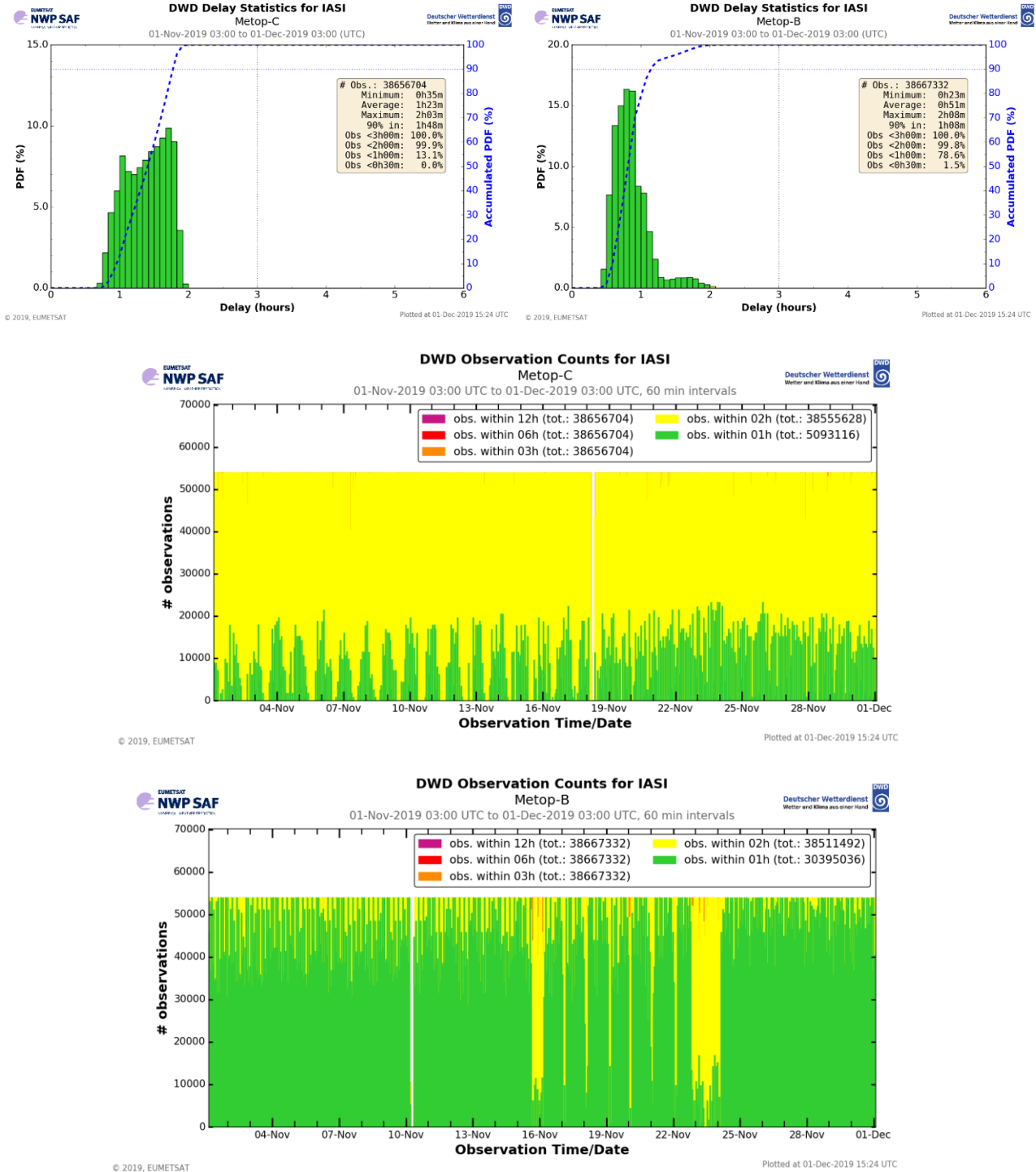
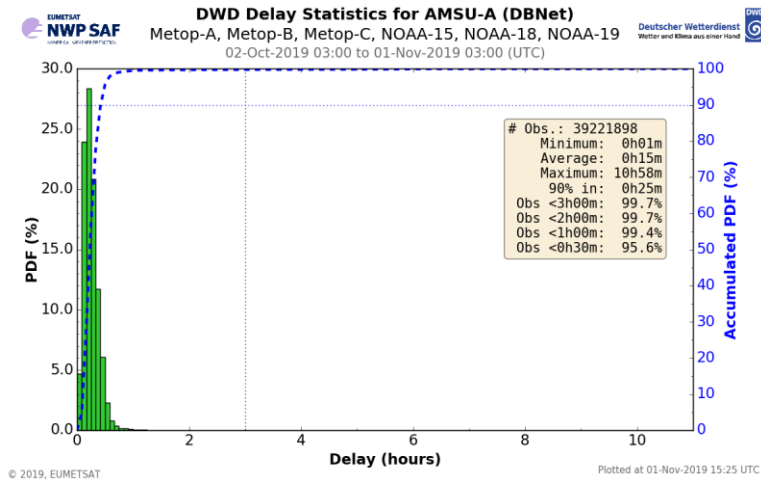


Figure 15: Monitoring of timeliness of IASI on Metop-C data for the period 1/11/2019-1/12/2019 from the DWD timeliness monitoring with timeliness defined as the elapsed time between observation time and entry time into DWD data base (received via EUMETCast transmission service);. Top left: PDF of timeliness for IASI on Metop-C top right: for IASI on Metop-B. Below: Timeseries of the number of data arriving within certain delay thresholds, middle: for IASI on Metop-C, bottom: for IASI on Metop-B.



DWD observation coverage AMSU-A (DBNet)
 01.11.2019 00 UTC

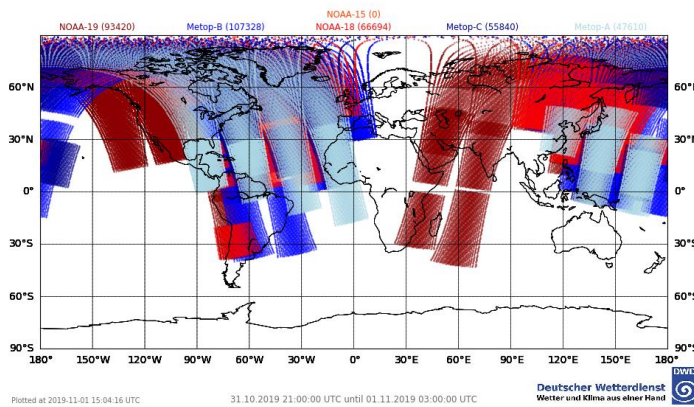


Figure 16: Top: Monitoring of timeliness of the fast data transmission service DBNet for AMSU-A data for all NOAA and EUMETSAT satellites (Metop-A, -B, -C and NOAA-15, -18, -19) for the month of October 2019.
 Bottom: Example of DBNet data coverage for AMSU-A from the 1 November 2019 for data from Metop-A, -B, -C and NOAA-15, -18, -19.